DOI:
10.1021/acs.langmuir.8b00866

Document Version
Peer reviewed version

Glycerol solvates DPPC headgroups and localises in the interfacial regions of model pulmonary interfaces altering bilayer structure

Journal:	*Langmuir*
Manuscript ID	la-2018-00866t.R1
Manuscript Type:	Article
Date Submitted by the Author:	08-May-2018
Complete List of Authors:	Terakosolphan, Wachirun; King's College London, School of Cancer and Pharmaceutical Sciences Trick, Jemma; King's College London, Department of Physics Royall, Paul; King's College London, School of Cancer and Pharmaceutical Sciences Rogers, Sarah; ISIS-STFC Neutron Scattering Facility, Harwell Science and Innovation Campus Lamberti, Olimpia; King's College London, Department of Physics Lorenz, Christian; King's College London, Department of Physics Forbes, Ben; King's College London, School of Cancer and Pharmaceutical Sciences Harvey, Richard; Martin-Luther-Universität Halle-Wittenberg, Institut für Pharmazie

Glycerol solvates DPPC headgroups and localises in the interfacial regions of model pulmonary interfaces altering bilayer structure

Wachirun Terakosolphan[1†], Jemma L. Trick[2†], Paul G. Royall[1], Sarah E. Rogers[3], Olimpia Lamberti[2], Christian D. Lorenz[2], Ben Forbes[1*], and Richard D. Harvey[4]

[1] *School of Cancer and Pharmaceutical Sciences, King's College London, London, SE1 9NH, UK*

[2] *Department of Physics, King's College London, London, WC2R 2LS, UK.*

[3] *Rutherford Appleton Laboratory, ISIS Facility, Chilton, Oxfordshire, OX11 0QX, UK.*

[4] *Institute of Pharmacy, Martin-Luther-University Halle-Wittenberg, Halle (Saale), 06099, Germany.*

[†] Equal contribution to first authorship

Corresponding Author

*ben.forbes@kcl.ac.uk

tel. +44 (0)207 848 4823

KEYWORDS: DPPC, glycerol, bilayer, monolayer, FTIR, Langmuir isotherms, Laurdan, SANS, molecular dynamics

ABSTRACT

The inclusion of glycerol in formulations for pulmonary drug delivery may affect the bioavailability of inhaled steroids by retarding their transport across the lung epithelium. The aim of this study was to evaluate whether the molecular interactions of glycerol with model pulmonary interfaces provide a biophysical basis for glycerol modifying inhaled drug transport. Dipalmitoyl-phosphatidylcholine (DPPC) monolayers and liposomes were used as model pulmonary interfaces, in order to examine the effects of bulk glycerol (0 – 30% w/w) on their structures and dynamics using complementary biophysical measurements and molecular dynamics (MD) simulations. Glycerol was found to preferentially interact with the carbonyl groups in the interfacial region of DPPC and with phosphate and choline in the headgroup, thus causing an increase in the size of the headgroup solvation shell, as evidenced by an expansion of DPPC monolayers (molecular area increased from 52 to 68 $Å^2$) and bilayers seen in both Langmuir isotherms and MD simulations. Both SANS and MD simulations indicated a reduction in gel phase DPPC bilayer thickness by ~3 Å in 30% w/w glycerol, a phenomenon consistent with the observation from FTIR data, that glycerol caused the lipid headgroup to remain oriented parallel to the membrane plane in contrast to its more perpendicular conformation adopted in pure water. Furthermore FTIR measurements suggested that the terminal methyl groups of the DPPC acyl chains were constrained in the presence of glycerol. This observation is supported by MD simulations, which predict bridging between adjacent DPPC headgroups by glycerol as a possible source of its putative membrane stiffening effect. Collectively, these data indicate that glycerol preferentially solvates DPPC headgroups and localises in specific areas of the interfacial region, resulting in structural changes to DPPC bilayers which may influence cell permeability to drugs.

INTRODUCTION

Glycerol (also known as Glycerin) is a small molecule which has a number of functions, such as plasticiser[1], humectant[2], and sweetener[3]. It is also included as a non-volatile excipient in some solution pressurised metered dose inhaler formulations to bulk drug particles, and tune the aerodynamic particle size distribution of emitted aerosols[4]. Respirable drug particles which contain both beclomethasone dipropionate (BDP) and glycerol show striking differences from solely BDP particles in terms of their biopharmaceutical properties; dissolution and drug transport. It has been shown that aerosol particles containing up to 50% w/w of glycerol dissolve more slowly and retard delivery of BDP across cultured pulmonary epithelial cell layers compared to glycerol-free formulations[5–7].

Pulmonary drug absorption is influenced by three vital interactions between an inhaled drug particle and the lungs; deposition, dissolution and permeability[8,9]. Lung penetration and deposition are highly dependent on the aerodynamic particle size of inhaled aerosols[7]. Upon deposition, drug particles encounter an air-interfaced DPPC-rich monolayer overlaying the mucosal surface of the airways or alveolar region[8,9]. Dissolution of poorly soluble drugs provides the rate-limiting step in the absorption of poorly soluble drugs from the lungs[9,10]. While the potential for excipients to modify drug dissolution is well known, this manuscript reports a mechanistic investigation into the proposition that glycerol may influence drug permeability by preferentially interacting with the lung surfactant layer and epithelial cell membranes. If a single emitted aerosol dose containing 250 µg glycerol deposited uniformly in the smaller airways of the lungs and dissolved in 20 mL lung lining fluid, a glycerol concentration 0.3% w/w would be generated (calculated according to the approach of Martinelli et al[11]); however hotspots of particle deposition and local concentration gradients around dissolving particles mean that a dynamic range of much higher glycerol

concentrations will be generated in practice, which is represented experimentally by 0 – 30% glycerol in our studies.

It is recognised that some pharmaceutical excipients that are commonly used in medicines and categorised as generally-regarded-as-safe by medicines regulatory agencies may exert unanticipated effects on drug permeability[12–14]. A number of permeation-enhancing mechanisms have been postulated including direct or indirect interference with membrane integrity, and interactions with enzymes or transporters, e.g. interactions of polyethylene glycol 400 with *in vitro* drug absorption models[12]. While the effects of excipients on drug permeability have been demonstrated functionally *in vitro* and enhancement of bioavailability has been demonstrated in humans, the biophysical or mechanistic explanations for these effects of excipients on biological barriers are vague and poorly defined. In contrast to agents that enhance permeability through increasing membrane fluidity[14], glycerol appears to stiffen membranes via molecular interactions that have not been fully resolved[15].

Dipalmitoylphosphatidylcholine (DPPC), as a major constituent of the lung pulmonary surfactant, can be used to model pulmonary interfaces for investigation of the effect of glycerol on lung surfactant and, when in the fluid phase, epithelial cell membranes. DPPC constitutes at least 40% of the lung's air-interfaced surfactant monolayer[16,17], and DPPC liposomes or monolayers are commonly used as a simple model of the epithelial cell plasma membrane[18–20]. The molecular interaction of glycerol (0 – 30% w/w) with DPPC and its effects on monolayer and bilayer structure were measured using a combination of Fourier transform infrared spectroscopy (FTIR), Langmuir pressure-area isotherms, small angle neutron scattering (SANS) and fluorescence-based membrane transition temperature determination. The putative stiffening effect of glycerol on DPPC is likely to be characterised by a stabilisation of the gel phase and therefore in order to investigate this

hypothesis, and to allow direct comparisons between this study and previously published work[15,21], we have concentrated on examining DPPC/glycerol interactions on gel phase lipids in the absence of salts. To complement the experimental studies, molecular dynamics (MD) simulations were used to investigate: (i) physical interactions between DPPC and glycerol, (ii) preferential localisation of glycerol in DPPC layers, and (iii) how glycerol affects the packing and conformation of DPPC molecules and bilayer dimensions, both in the gel and fluid phases in physiological saline to represent the effects of glycerol interactions with membrane lipids.

We postulate that the retardation of the absorptive transport of BDP by glycerol observed *in vitro*[5,7] may result in part from an excipient-induced reduction in membrane fluidity. Accordingly, the aim of this study was determined how glycerol interacts structurally and sterically with model pulmonary interfaces using the combination of biophysical experimental and simulation approaches described above.

EXPERIMENTAL SECTION

Materials. 1,2-dipalmitoyl-*sn*-glycero-3-phosphocholine (dipalmitoylphosphatidylcholine; DPPC, purity > 99%) and 1,2-dipalmitoyl-d_{62}-*sn*-glycero-3-phosphocholine (d_{62}DPPC, purity > 99%) were purchased from Avanti Polar Lipids (Alabaster, AL, USA) and used without further purification, 6-dodecanoyl-N,N-dimethyl-2-naphthylamine (Laurdan) was obtained from Molecular Probes (Eugene, OR, USA), chloroform from Fisher Scientific (UK), and glycerol (purity > 99%) from Sigma-Aldrich (London, UK). Ultrapure water with 18.2 MΩ·cm residual specific resistance was obtained using an Elgastat Maxima purifier (Elga, UK). All other reagents were obtained from standard sources.

Methods. ***Preparation of DPPC liposomes.*** Liposomes were formed using the thin film resolvation technique by first dissolving 10 mg of DPPC in chloroform, which was removed by evaporation at room temperature in a vacuum desiccator overnight to obtain thin dry lipid films deposited on the inside walls of glass vials. The dried lipid films were resolvated in ultrapure water and various concentrations of glycerol solution (1.0 – 30.0% w/w) to achieve a final DPPC dispersion concentration of 4 mg/mL. The liposomes were ultrasonicated using a Soniprep 150 ultrasonic probe disintegrator (MSE, UK) at an amplitude of 10 microns for 5 minutes (to minimise the effect of metal particles shed from the tip), and were allowed to anneal at room temperature prior to further use.

Fourier transform infrared spectroscopy. To scan the interferogram, solvent without DPPC (either ultrapure water or 1.0 – 30.0% w/w glycerol solutions) and liposome dispersion droplets were separately placed using a micropipette, on an attenuated total reflection (ATR) crystal surface attached at an ATR accessory sample compartment (Specac, Kent, UK) as background and sample, respectively. Infrared spectra were obtained using a Spectrum One FTIR spectrometer (Perkin-Elmer, USA), operated with Spectrum software (version 5.3.1) under ambient conditions at 23°C. Interferograms were collected for a wavenumber range from 4000 to 600 cm^{-1} and averaged for 128 scans at 4 cm^{-1} resolution. Data processing consisted of baseline smoothing using the automatic smooth processing function in the Spectrum software.

At a region from 3000 to 2800 cm^{-1}, the frequencies of the CH_2 symmetric stretch were estimated to the nearest 0.1 cm^{-1} at 80% of peak height. The frequencies of the carbonyl group (C=O) stretching were obtained from the major peak absorbance of a region from 1800 to 1600 cm^{-1}. Lastly, the frequencies of the phosphate (PO_2^-) and the choline ($N(CH_3)_3^+$) asymmetric stretches were measured to the nearest 0.1 cm^{-1} from the peak absorbance of these bands, within

the 1240 to 1220 cm^{-1} and approximately 970 cm^{-1} region, respectively[22,23]. The spectral changes associated with these vibrational modes are of characteristic value, since they can provide valuable structural and conformational information about the changes which occur in the acyl chains, interfacial region (ester carbonyls) and the headgroup (phosphate and choline moieties) of the lipid molecules[22].

Surface pressure; area isotherms of air/liquid interface monolayers. DPPC monolayer pressure-area isotherm measurements were carried out at 23°C on a Nima 602A Langmuir trough (Nima Technologies Ltd., Coventry, UK) equipped with a Nima PS4 microbalance (0 – 240 mN/m range, 0.1 mN/m resolution) controlled by a PC equipped with the Nima IU4 computer interface unit software. A clean Wilhelmy plate (Whatman 1 CHR chromatographic paper, of 20.36 mm perimeter, GE Healthcare life sciences UK, Little Chalfont, UK) which was washed in chloroform before use was attached to the microbalance, suspended and submerged in the subphase (either ultrapure water or glycerol solution).

A 1 mg/mL DPPC solution in chloroform (40 μL) was spread onto the subphase surface by dropwise addition using a Hamilton syringe (Hamilton Co. Europe, Bonaduz, Switzerland), with the trough barriers open at their maximum area. The resultant monolayer was allowed to stand for 15 min to ensure the complete evaporation of chloroform before compressing the barriers at a constant rate of 35 cm^2/min. During the compression, changes in the surface pressure were recorded in the form of surface pressure (mN/m) against mean area per lipid molecule ($Å^2$/molecule) until the monolayer reached its collapse point, in triplicate. From the isotherms produced, the hypothetical area occupied by one phospholipid molecule in the well oriented and closely packed monolayer could be indicated from interpolating the molecular area for a surface pressure of 30 mN/m which is considered as the biological surface tension of lung surfactant in

the human conducting airways[24]. In addition, the surface compressional modulus *(K^s)*, which gives a measure of the elasticity of the monolayer, was calculated for the condensed phase of the isotherms using:

$$K^S = -A \times \left(\frac{d\pi}{dA}\right) \qquad (1)$$

where A is the area per molecule and $d\pi/dA$ is the slope of the isotherm[25].

Fluorimetric measurement. Liposomes were prepared as described above, with a small amount of the fluorescent probe Laurdan added into the DPPC-chloroform solution to give a total lipid/Laurdan molar ratio between 300:1 and 400:1 prior to solvent evaporation and resolvation in water or glycerol solution. In order to limit photo bleaching of the Laurdan the sample vials were protected from light with aluminium foil during liposome preparation[26].

Steady-state Laurdan fluorescence emission was measured using a Varian Cary Eclipse spectrofluorimeter (Agilent, USA) using a 104F-QS semi-micro dual light path (10 × 4 mm) fluorescence cell (Hellma Analytics, Germany). Fluorescence spectra were recorded over a temperature range from 25°C to 65°C increasing in 5°C increments. The temperature of the sample compartment was adjusted using a water-circulating thermostat-controlled Varian Cary Single-Cell Peltier Accessory (Agilent, USA). The temperature inside the cuvette was directly measured with a K-thermocouple thermometer HI 935005 (Hanna, USA). Emission intensities of all samples were acquired with an excitation wavelength of 340 nm, adjusted for optimal spectral intensity with an excitation slit width of 10 nm and an emission slit width of 5 nm, and scanned from 360 nm to 560 nm. Afterwards, the generalised polarisation (GP) was calculated using the fluorescence intensities at the maximum emission wavelengths of Laurdan exhibited when mixed with lipids in

either their gel (I_g) or liquid-crystalline (I_c) phases, in this case 440 and 490 nm are used respectively, according to the formula[27,28].

$$Generalised\ polarisation = \frac{I_g - I_c}{I_g + I_c} \qquad (2)$$

The generalised polarisation as determined using equation (2) was plotted against temperature and the resultant sigmoidal curve was fitted to a 4-parameter logistic model using SigmaPlot version 13.0. After fitting the GP curve, the main phase transition temperature for each sample was obtained from the inflection point of the fitted sigmoidal curves[29].

Small angle neutron scattering. The SANS measurements were carried out on the LoQ small-angle diffractometer at the ISIS pulsed neutron source (STFC Rutherford Appleton Laboratory Oxon, U.K.)[30,31]. LoQ is a fixed-geometry "white beam" time-of-flight instrument which utilises neutrons with wavelengths in the range of 2.2 – 10 Å. Data are recorded on a positive sensitive neutron detector to provide a simultaneous Q-range of 0.008 – 0.3 $Å^{-1}$. Each raw scattering data set was corrected for the detector efficiency; sample transmission and background scattering (water or glycerol solution) and converted to scattering cross-section data using the instrument-specific software[32]. These data were placed on an absolute scale (cm^{-1}) using the scattering from a standard sample (a solid hydrogenous and perdeuterated polystyrene) in accordance with established procedures[33].

Liposomes were prepared as described above, using chain-deuterated d_{62}DPPC. The dried lipid films were resolvated using ultrapure to form two samples, one in water (0%) and one in a 30% w/w glycerol solution each containing a final d_{62}DPPC concentration of 2 mg/mL. The samples were placed in cleaned quartz cells of 1 mm path length, and the scattering pattern was recorded at 25°C for approximately 4.5 hours each. The data were analysed by fitting the experimental

scattering curves to the mathematical model describing stacked random lamellar sheets with a paracrystalline structure factor[34], using the DANSE SasView software (version 4.0)[35]. During the fitting process, a range of physically reasonable background scattering intensities were introduced into the calculations according to theoretical values for the solvents.

Molecular dynamics simulation. DPPC monolayers and bilayers containing ~150,000 and 400,000 atoms, respectively, were constructed via the CHARMM-GUI membrane builder[36]. These "boxes" were used to build systems with glycerol concentrations of 0, 10, 20 and 30% (percentage based on water-weight and the number of water molecules within the simulation system) within the aqueous phase. The solvent phase also contained 0.15M NaCl in solution. Due to simulation box sizes (based on the thickness or width of water present between the leaflets), the number of lipids varied in the systems for the different glycerol concentrations (300 for 0 and 10, 400 for 20 and 600 DPPC lipids for 30%). All simulations were carried out using GROMACS (www.gromacs.org) version 5.0.7[37] using the CHARMM36 force field[38]. Each system was simulated at temperatures of 310, 314, 316 and 323, and treated with a Nose-Hoover thermostat[39] coupled to a constant $\tau_T = 0.1$ ps.

Monolayer simulations were carried out via the NVT (constant Number of atoms, Volume and Temperature) ensemble, and bilayers via the NPT (constant Number of atoms, Pressure and Temperature) ensemble using a Parrinello-Rahman barostat[40] at $\tau_p = 1$ ps. Equilibrium simulations were simulated with long-range electrostatic interactions treated using the Particle Mesh Ewald method[41] with a short-range cutoff of 1 nm and a Fourier spacing of 0.12 nm. Each production simulation was 100 ns in duration (unless otherwise stated). Analysis was conducted using in-house code and MDAnalysis[42].

Statistical analysis. Statistical analysis of the experimental data was performed using SPSS version 23 with a minimal level of significance of 0.05. One-way analysis of variance (ANOVA) was employed to analyse the data, and post hoc comparisons of the means of individual groups were performed using Scheffe test.

RESULTS

Fourier transform infrared spectroscopy. FTIR spectra of DPPC MLVs in solutions of various concentrations of glycerol are shown in figure 1. The characteristic absorption band peaks of samples at the CH_2 symmetric stretch, carbonyl stretching, phosphate and the choline asymmetric stretch regions were distinct and showed differences between the liposomes dispersed in the different glycerol solutions.

The methylene (CH_2) and the terminal methyl (CH_3) stretching modes of the palmitoyl chains were used to investigate the structural changes within the lipophilic part of the bilayer[23]. When the palmitoyl chains are ordered (all-trans) they exhibit a frequency of ~2851 cm^{-1}, whereas disordered (melted; gauche) chains exhibits a higher frequency (~2853.5 cm^{-1})[43]. The presence of glycerol does not change the conformation of the acyl tails, the principal peaks obtained from the DPPC MLVs in solutions with various concentrations of glycerol (0 – 30% w/w) presented with very similar wavenumbers at 2850.4 cm^{-1}, suggesting that the presence of glycerol has little effect on acyl chain conformation. The changes in the vibrational frequency of the terminal methyl asymmetric stretching band reflects the stiffness of the central area of the bilayers. A shift to a higher wavenumber in this band implies increasing flexibility of the bilayers, and *vice versa*, a shift to a lower wavenumber reflects a stiffer bilayer[22,23]. The addition of glycerol decreased the wavenumber of this band from 2956.3 cm^{-1} (0%) to 2955.2 cm^{-1} (10% w/w glycerol), then

remained at approximately 2955.3 cm^{-1} (30% w/w glycerol, table 1) indicating that the mobility of terminal methyl at the central core of DPPC bilayers was restricted.

The effect of glycerol and its interactions at the interfacial and polar region of DPPC bilayers, was assessed by examining changes in the C=O stretching bands arising from the ester carbonyls (attributable to hydrogen-bonded carbonyl groups). At this region, a shift to higher wavenumbers implies little or no hydrogen bonding and a shift to lower wavenumbers suggests that there is an increase in hydrogen bonding[22]. The addition of glycerol into DPPC MLVs results in an increase in the wavenumber for the C=O stretching modes (table 1) with a shift in vibrational frequency from 1732.7 cm^{-1} (0%) to 1738.9 cm^{-1} (30% w/w glycerol), indicating a dehydration of the carbonyl groups.

Both the PO_2^- and the $N(CH_3)_3^+$ antisymmetric stretching bands of the DPPC headgroup can be used to indicate their level of hydration[44]. The phosphates that are hydrogen-bonded to water exhibits a maximum wavenumber of 1222 cm^{-1} in the fully hydrated state, and shifts towards higher wavenumbers (~1243 cm^{-1}) when dry[45]. Accordingly, the wavenumber for the phosphate stretching bands fluctuated between 1222.5 cm^{-1} and 1224.5 cm^{-1}, in response to the addition of glycerol, implying that the phosphate groups remained close to full hydration. On the other hand, an increase in the frequency of the choline stretching band was observed (from 971.1 to 973.9 cm^{-1}, table 1). Regarding this region, a shift to a higher wavenumber of the $N(CH_3)_3^+$ asymmetric stretching indicates increased hydrogen bonding at the choline group[46] and a change of the choline orientation such that it is bending towards the surface plane of the bilayer[47], caused by the presence of glycerol.

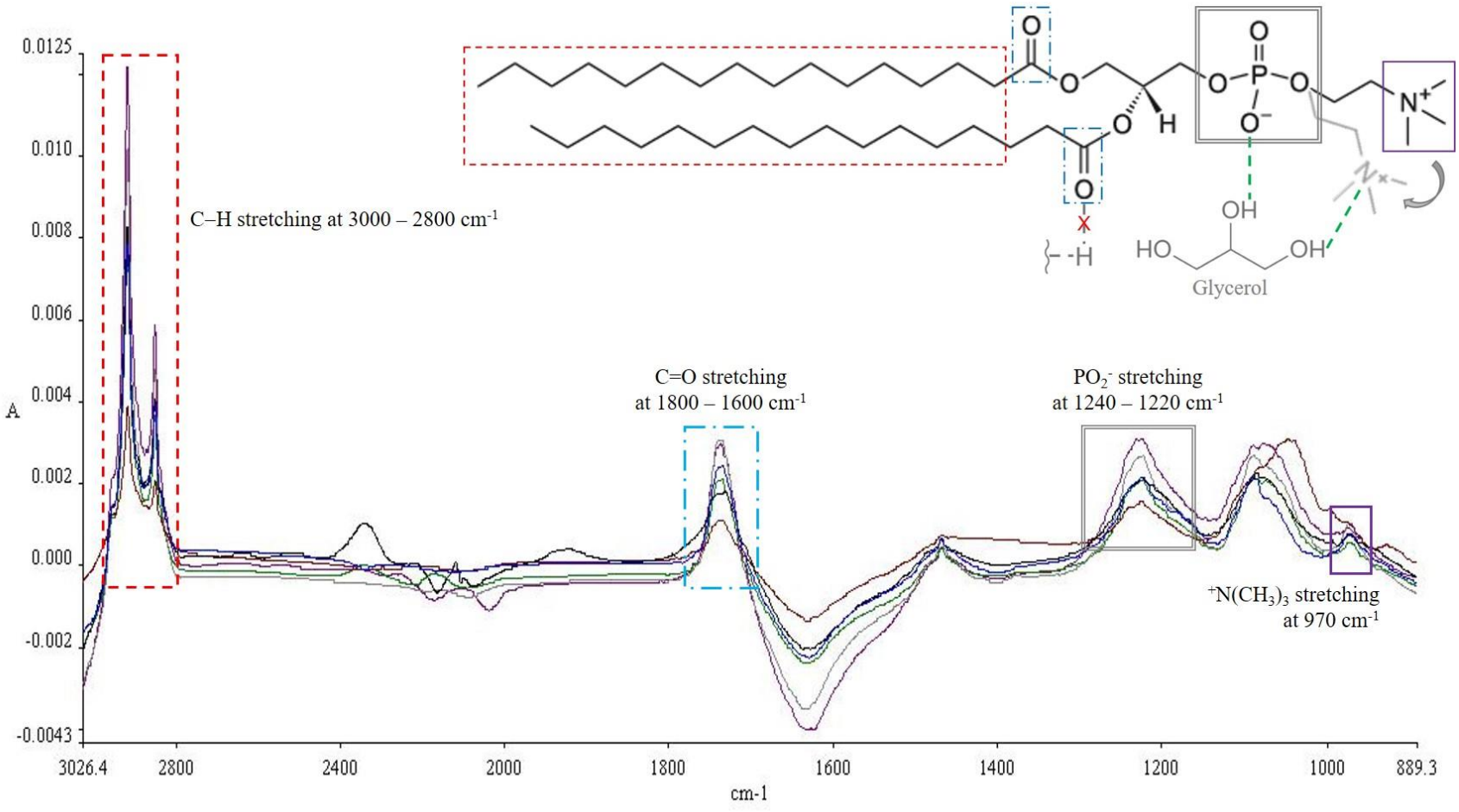

Figure 1. FTIR spectra of DPPC liposomes in the following concentrations of glycerol solution, measured at 23°C: black − 0%, blue − 1.0%, violet − 5.0%, green − 10.0%, grey − 20.0%, and brown − 30.0%. Specific regions of the FTIR spectra for each moiety of DPPC molecule are indicated. Inset shows the proposed effects of glycerol on DPPC molecule; dehydration at the interfacial carbonyl, hydrogen-bonds with phosphate and choline in the headgroup, and change in the choline orientation.

Table 1. Changes in the vibrational frequency of three specific regions of DPPC molecules in liposomes dispersed in various concentration of glycerol, measured at 23°C.

Glycerol (% w/w)	Wavenumber (cm^{-1})		
	CH_3 stretching	C=O **stretching**	**$N(CH_3)_3^+$ stretching**
0	2956.3 ± 0.1	1732.7 ± 0.6	971.1 ± 1.0
1	2955.7 ± 0.3	1736.4 ± 2.0	971.5 ± 0.6
5	2955.4 ± 1.2	1738.1 ± 1.7	972.4 ± 0.5
10	2955.2 ± 0.3	1738.5 ± 0.6	972.8 ± 2.6
20	2955.3 ± 0.4	1738.9 ± 0.3	973.3 ± 2.0
30	2955.3 ± 0.4	1738.9 ± 0.3	973.9 ± 1.3

Surface pressure; area isotherm of air/liquid interface monolayers. From the monolayer isotherm measurements shown in figure 2, there is an evident effect of increasing subphase glycerol concentration on the area per molecule (APM) of DPPC across the full range of surface pressures.

From the pressure-area isotherms measured for each DPPC monolayer (with different glycerol concentrations, and therefore differing surface tensions ranging from 71.9 mN/m in pure water to 68.5 mN/m in 30% w/w glycerol at 25°C[48]) different behaviours were observed during monolayer compression. In pure water, the surface pressure-molecular area isotherm for DPPC has a lift off from the gaseous phase at ~114 $Å^2$ and appears to enter a transition into a coexisting liquid expanded (LE) – liquid condensed (LC) phase at around 5 mN/m. Beyond this point, the surface pressure rises sharply and exhibits characteristics of an LC phase monolayer, until it collapses at ~55 mN/m (giving a limiting APM of 44 $Å^2$). Interestingly, the rightward shift observed for the DPPC isotherms on subphases with increasing glycerol concentration, exhibit a cluster of lift-off points from 130 – 150 $Å^2$, suggesting that the lipids begin to interact at increasingly lower surface

densities, which may be attributed to interactions associated with headgroup solvation shells[15]. The phase transition at ~5 mN/m visible in the isotherms of DPPC on pure water, are absent from the isotherms obtained on glycerol solutions >10% w/w.

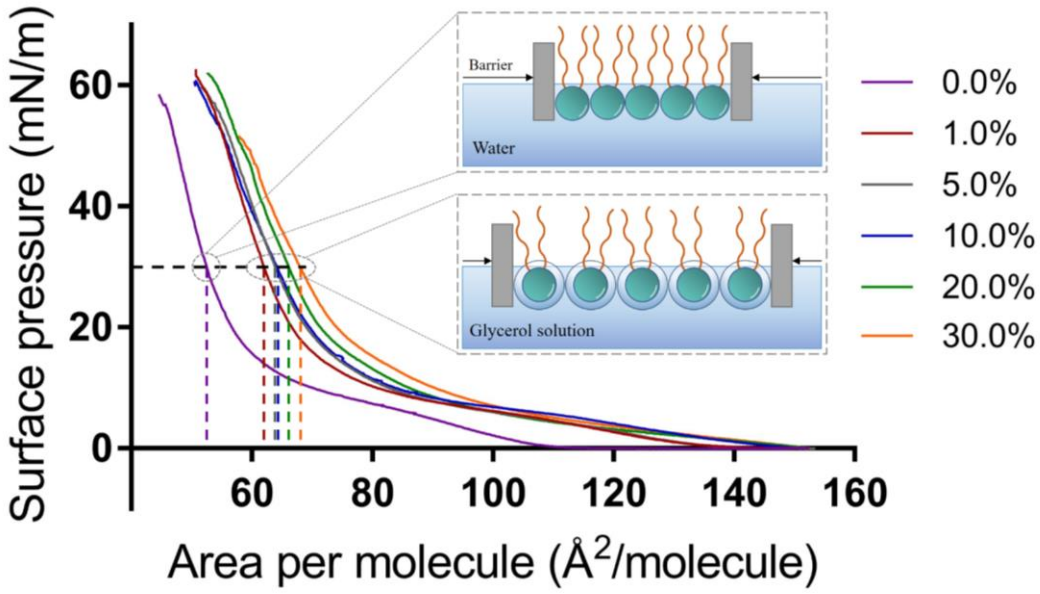

Figure 2. Surface pressure-area isotherms of DPPC monolayer on subphases containing various concentrations of glycerol (0 – 30% w/w), measured at 23°C. The dashed lines represent the mean area per molecule for each sample at 30 mN/m. Inset illustrates the proposed phenomena of DPPC monolayers on both glycerol-free and glycerol-containing subphases in which the solvation shell of the lipid headgroups is enriched with glycerol.

The mean area per molecule for the DPPC monolayers also showed a rightward shift in response to increasing glycerol concentration in the subphase. Taking the mean APM at 30 mN/m as a comparator, they increase from 52.5 Å^2 in pure water, to 68 Å^2 in 30% glycerol (table 2). The results suggest that the presence of glycerol in the subphase significantly increases the size of the phosphocholine headgroup solvation shell ($p < 0.001$) thus facilitating steric interactions between adjacent lipid molecules at lower surface pressures.

Table 2. Changes in the mean area per molecule of DPPC and the surface compressional modulus of DPPC monolayers at 30 mN/m on subphases containing various concentration of glycerol at 23°C.

Glycerol (% w/w)	Mean area per molecule (Å^2)	Surface compressional modulus (mN/m)
0	52.5 ± 1.5	211.0 ± 8.3
1	62.1 ± 2.3	198.7 ± 21.2
5	63.8 ± 2.0	181.3 ± 11.0
10	64.2 ± 2.0	158.4 ± 10.9
20	66.1 ± 1.0	170.3 ± 12.8
30	68.0 ± 1.1	157.2 ± 16.0

For further insight, the surface compressional moduli were determined form the isotherms in order to determine the effect of increasing glycerol concentration on the elasticity of the lipid monolayers. This parameter was calculated from the tangent of the isotherms at 30 mN/m using equation (1). Table 2 shows that the overall trend of the calculated surface compressional moduli for the DPPC monolayers is one of incremental decrease as the glycerol concentration increases (10 – 30% w/w compared to that from the glycerol-free control sample; $p < 0.05$), although the magnitude of these changes is comparatively small, as the K^s values for all of the monolayers fall well within the range expected liquid condensed (LC) phases[25].

Fluorimetric measurements. The fluorescence emission spectra (figure 3A) for Laurdan in multilamellar DPPC vesicles at temperatures varying from 25°C (corresponding to the gel phase of DPPC) to 65°C (the liquid crystalline phase) measured in ultrapure water, show that during the phase transition, the spectral peaks shift to longer wavelengths. The Laurdan emission spectrum

for liposomes in the liquid crystalline phase (high temperatures) shows a decrease in intensity at longer wavelengths with respect to the spectrum observed in the gel phase (low temperatures). These differing emission maxima intensities for Laurdan mixed with gel and liquid crystalline phase lipids (440 and 490 nm respectively) were used to calculate the Laurdan generalised polarisation (GP) using equation (2).

The temperature dependence of Laurdan GP for DPPC MLVs dispersed in H_20 (0%) and 30% w/w glycerol solutions is shown in figure 3B. As anticipated, the GP decreased from about 0.5 at temperatures corresponding to the gel phase to -0.35 for the liquid crystalline phase. The main phase transition temperature of the glycerol-free system lies within the range previous determined for pure DPPC (41.5°C)[28]. In the presence of glycerol, the measurements showed a similarity in the GP for the temperature ranges from 25 to 35°C and from 45 to 65°C at all glycerol concentrations (see Supporting Information figure S1). However, an increase in the GP in the glycerol-containing liposomes over the range of the phase transition temperature, approximately at 35 to 45°C, was detected. It can be implied that the glycerol-containing membrane required slightly a higher temperature to induce chain melting, and then allow solvent molecules to penetrate the headgroup of the lipids and interact with the Laurdan.

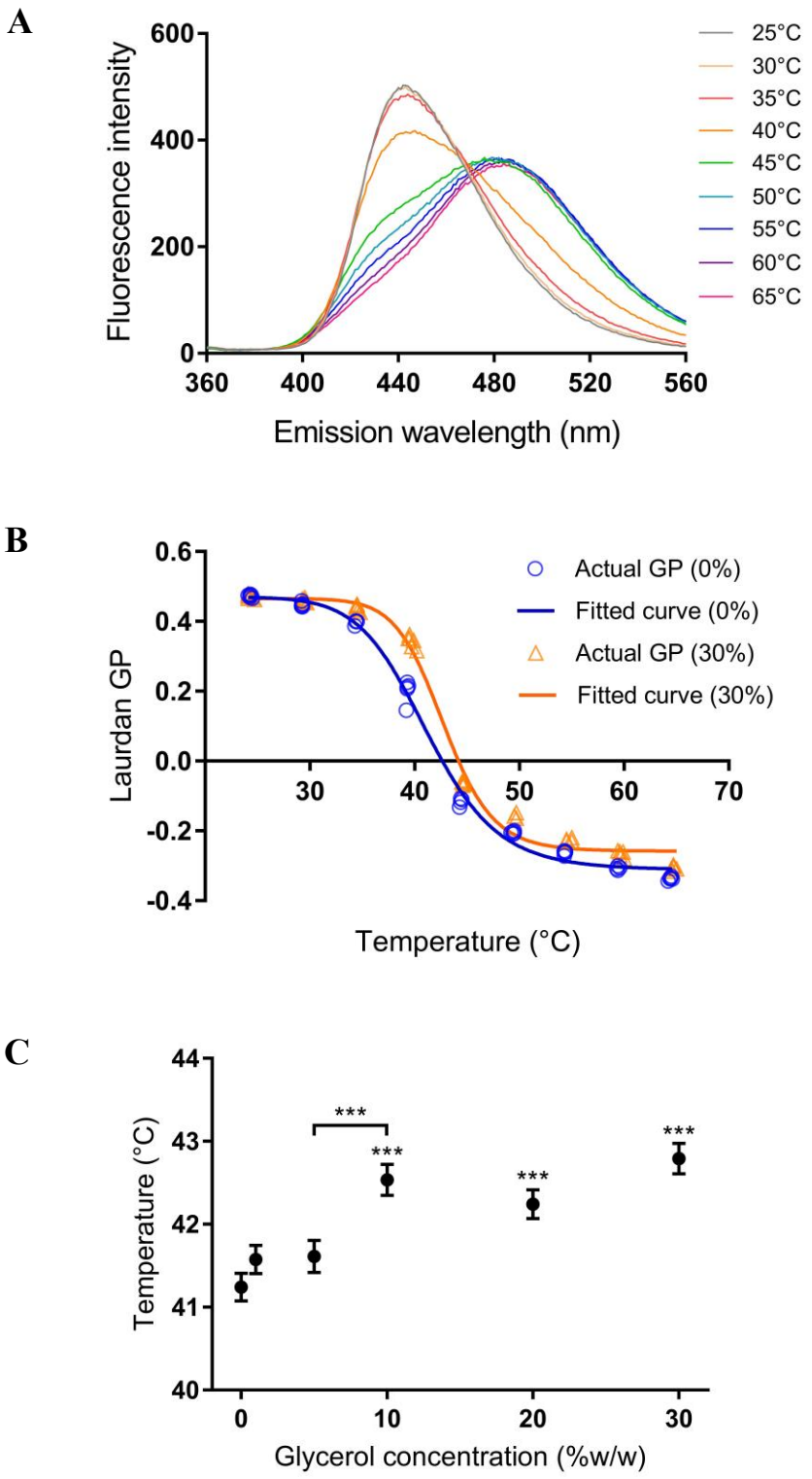

Figure 3. (A) Fluorescence emission spectra for Laurdan in DPPC multilamellar vesicles at different temperatures, measured after excitation at 340 nm in ultrapure water. **(B)** Temperature

dependence of the effect of 30% w/w glycerol on the Laurdan GP in DPPC MLVs. **(C)** Estimated gel to fluid phase transition temperature (T_m) of DPPC MLVs in varying glycerol concentrations. Data were obtained from the temperature at the inflection point of each fitted GP curve (see Supporting Information). The significance level accepted, $^{***}p$-value < 0.001.

The estimated phase transition temperatures obtained from the inflection point of the fitted GP curves of DPPC MLV in 0, 1, 5, 10, 20, and 30% w/w glycerol solutions (see Supporting Information figure S1) were 41.2°C, 41.6°C, 41.6°C, 42.5°C, 42.2°C, and 42.8°C respectively, thus indicating a slightly increasing transition temperature as the percentage of glycerol increases, and significant differences compared to the glycerol-free control sample were noted (figure 3C). The T_m of the glycerol-containing liposomes at 10 – 30% w/w were significantly different from the control, furthermore, the multiple comparison using the Scheffe test shows a significant step change in T_m between 5 and 10% w/w glycerol.

Small angle neutron scattering (SANS). The scattering curves obtained from dispersions of d_{62}DPPC in both H_2O (0%) and 30% w/w glycerol solution (see Supporting Information figure S2), were mathematically fitted with a paracrystalline lamellar stack model[34] (table 3). The neutron scattering length density (SLD) values for the d_{62}DPPC and solvents used for the fitting, were obtained directly from scientific literature or calculated using published molecular density and atomic scattering length values[15,49,50].

The bilayer parameters obtained from the fitted scattering curves (table 3) show small, but significant differences between the vesicles dispersed in pure H_2O and those in the 30% w/w glycerol solution. In both cases, the scale factors (volume fraction of the lipids in the samples) and background scattering values are similar, with the Chi-squared value indicating that the error of the fitting is low implying a valid fit. The sonication method employed to make the samples usually

produces a mixed population of vesicle morphologies, including unilamellar (ULV), multilamellar (MLV) and oligolamellar vesicles (OLV)[51], which may have influenced the values obtained for the bilayer parameters.

Table 3. Bilayer parameters obtained from fitting SANS curves for d_{62}DPPC in both H_2O (0%) and 30% w/w glycerol solution, with the paracrystalline lamellar stack model using DANSE SasView[35].

Fitted parameter	d_{62}DPPC (water)	d_{62}DPPC (30% glycerol)
Scale factor	0.1	0.1
Layer thickness (Å)	38.8 ± 0.6	35.7 ± 0.5
Number of layers	1.5 ± 0	1.4 ± 0
Stack d-spacing (Å)	59.2 ± 0.5	58.4 ± 0.3
Sigma d	2.01×10^{-5}	2.93×10^{-7}
SLD of layer (Å^2)	5.62×10^{-6}	5.55×10^{-6}
SLD of solvent (Å^2)	-5.60×10^{-7}	8.99×10^{-8}
Background (cm^{-1})	0.0011	0.0011
Chi-squared	20.9	14.6

Fitting the data as single lamellar sheets does not yield physically plausible bilayer parameters, implying the presence of some lamellar stacking within the samples. For both samples, the d-spacings obtained from the model fits (59.2 ± 0.5 Å, 0% and 58.4 ± 0.3 Å, 30% w/w glycerol) (the sum of the bilayer thickness and the thickness of the water layer separating stacked bilayers) are slightly lower than the value of 63.5 Å previously obtained for gel phase DPPC bilayers by X-ray diffraction measurements[52]. The proportion of stacked bilayers appears to be low (approximately 1.4 in each sample), which could have had a small effect on the accuracy of the d-repeat spacing and its variance (Sigma d). As the d_{62}DPPC used to make the samples possessed only deuterated

acyl chains, the highest scattering contrast existed between the solvent and the chains implying that the layer thickness obtained from the fits represents the thickness hydrophobic region. Thus, the ~39 Å layer thickness value obtained in H_2O (0%) is lower than the phosphate to phosphate thickness obtained by X-ray diffraction (44.2 Å)[52], however it is of similar magnitude as the theoretical hydrophobic region thickness calculated for gel phase DPPC (~37.5 Å)[53].

A small decrease in the hydrophobic layer thickness is observed in the vesicles dispersed in 30% w/w glycerol (35.7 Å), when compared to those in water (0%, 38.8 Å) however this decrease is not of the magnitude observed during a phase transition (gel to fluid) for DPPC (~6 – 10 Å change in hydrophobic thickness)[52]. This, together with the small change in SLD modelled for the lipid layers in water and glycerol solution implies that the layer thickness change may be due to alterations in lipid packing or headgroup orientation, arising from interaction with the glycerol.

Molecular dynamics simulation (MD).

Investigation into Specific Glycerol-Water-DPPC Interactions

In the simulated systems, the glycerol is observed to be evenly distributed throughout the bulk of the solvent (as shown in the density plot in figure 4A and the snapshot of the simulated system in figure 4B). The glycerol molecules do not appear to penetrate the membrane to the same extent as the water molecules do. Instead, visual inspection of snapshots from the simulation trajectories informs us that the glycerol preferentially interacts with the lipid head groups (as shown in the snapshot shown in figure 4C). As a result, the interaction between the glycerol molecules and the lipid head groups are quantified in the remainder of this section.

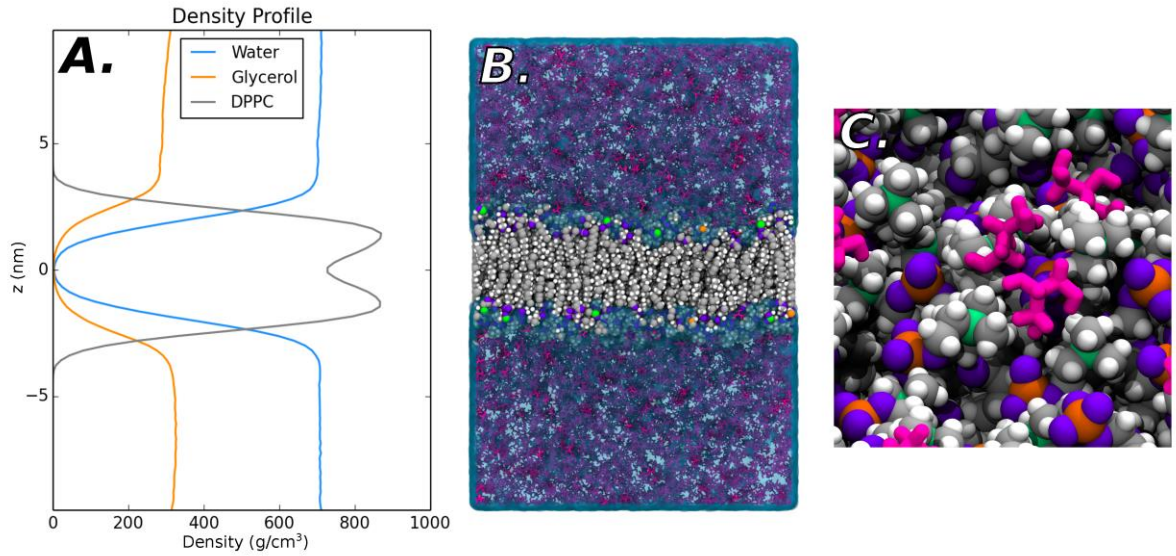

Figure 4. (A) Density profile as a function of the z-dimension for the DPPC (grey), water (blue) and glycerol (orange) for the 30% glycerol system at T = 323 K, **(B)** Snapshot of an equilibrated DPPC bilayer in the solvent containing 30% glycerol at T = 323 K (lipids = grey, water = light blue, glycerol = purple). **(C)** Snapshot showing how glycerol (shown in pink cylinder representation) interacts with the onium group of the DPPC molecules in the bilayer (nitrogen in onium group of DPPC = green; carbons in onium group of DPPC = grey; hydrogens in onium group of DPPC = white; chloride ions = purple).

The hydrogen bonding numbers analysed from simulation are in agreement with the carbonyl/C=O stretching from experimental FTIR data presented (table 1 and figure 1 previously), suggesting a dehydration event, accompanied by an increase in hydrogen bonding with the hydroxyl region of glycerol (figure 5). Data collated from simulation also suggests an increase in hydrogen bonding to the phosphate-oxygen atoms (figure 5). However, a significant change within the phosphate dehydration/hydration was not seen in the experimental FTIR data, thus could be an

artefact of the simulation here, or possibly a smaller event within FTIR in comparison to the rest of the lipid molecule.

From the bilayer simulations, it can be noted that glycerol prioritises hydrogen bonding to the double-bonded carbonyl oxygen atoms of the DPPC molecule, and has a higher bonding propensity to the phosphate oxygen atoms (seen from the substantially larger number of hydrogen bonds within figure 5). Interestingly, the number of hydrogen bonds (the sum of those made with the ester carbonyls and phosphate groups of the lipid) does not drastically change with the change in temperature (310 and 323 K). Thus, this may have a minimal role in the small change in lipid transition temperature noted previously.

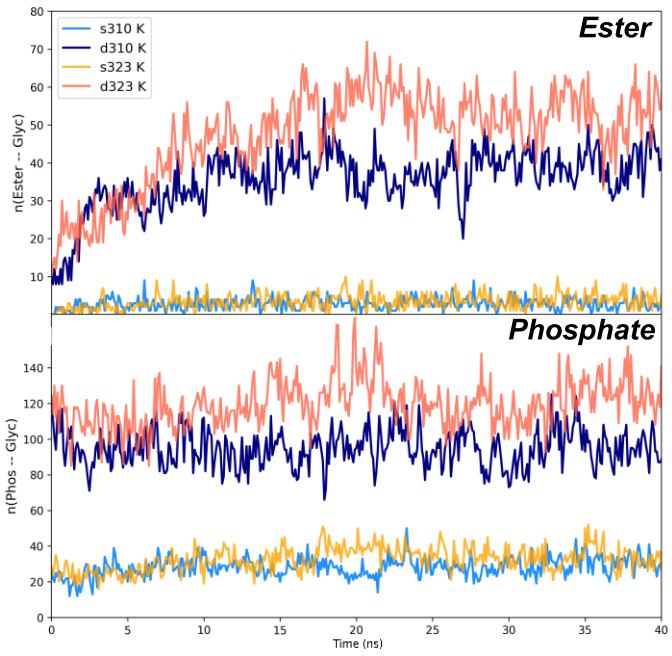

Figure 5. Hydrogen bonding numbers of ester carbonyl oxygen atoms (top, ester region) and phosphate oxygen atoms (bottom plot, phosphate group) to glycerol for a bilayer simulation. The "single" (main chain oxygen atom for ester and phosphate groups, s310 & s323) or "double" bonded oxygen atoms (carbonyl oxygen for ester and not the main chain oxygen atoms within the

phosphate moiety, d310 & d323) at 310 K and 323 K are indicated in the figure. Hydrogen bonds are identified as those donor and acceptor groups which are within 3.5 Å of one another and have bonds which make a 45 degree angle with one another.

From simulation, the location of the permeating glycerol molecules into the DPPC can be quantified by treating the surface of DPPC as an intrinsic surface[54] in which the chemical groups of the lipid can be thought of as differing layers. Thus instead of gaining an overall estimate of the depth and location of a molecule (like conventional density plot methods), a more precise location of the molecule can be analysed and the location of the glycerol molecule can be described in detail. In the 30% w/w glycerol simulations, the glycerol molecules interact with the outer region of the DPPC lipid (between the choline and ester carbonyl groups, indicated as grey bars in figure 6A) as anticipated (from the density gradient of glycerol from the water). From there, as one would expect if there were non-preferential interactions, the next highest region would be between the choline and the phosphate groups which are closest to the water region. However from intrinsic surface calculations, the glycerol molecules are present in a higher number between the phosphate and the ester carbonyl region than are found just below the choline group itself. From here, the next range of contacts are made between the choline and the phosphate region of the lipid (indicated as orange, purple, and then green bars in figure 6A). These locations of glycerol suggest that there may be specific interactions between the ester carbonyl region and glycerol molecules, resulting in a higher localisation of glycerol in this region than below and above the ester groups.

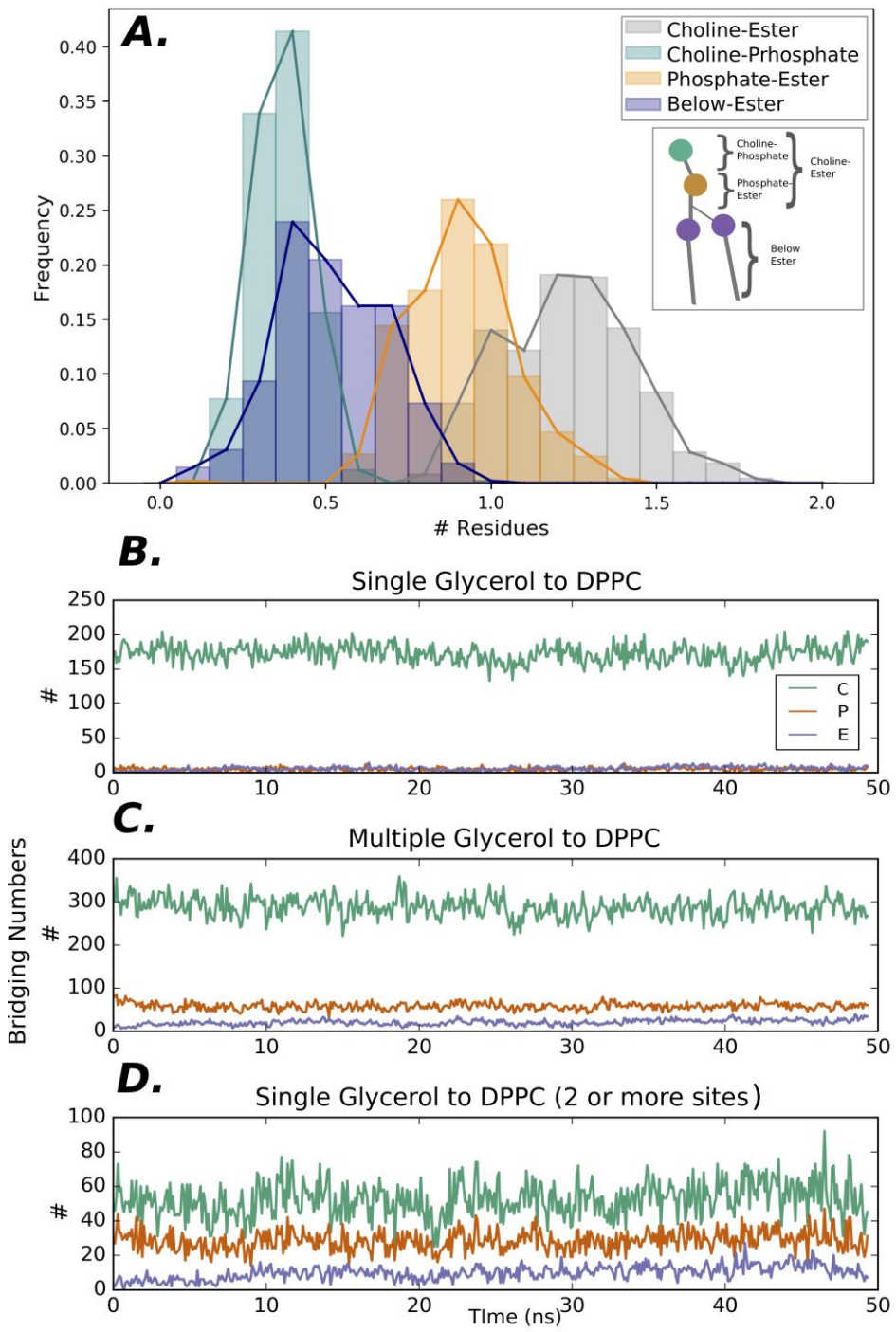

Figure 6. (A) Plot of the number of glycerol interactions with a DPPC lipid within the intrinsic surface layer. "Layers" of the lipid are indicated within the inset figure in corresponding colours with the green bead indicating the choline group, orange phosphate, and purple the ester carbonyl (to mark as boundaries between). **(B)** The number of glycerol molecules bound to the three

different regions of the lipid headgroup over the course of the simulation. **(C)** Number of glycerol molecules bound to different regions of lipid headgroup when more than one glycerol is present around a lipid molecule over the course of the simulation. **(D)** Number of lipids that bind to the different regions of the headgroup when bridging two lipid molecules over the course of the simulation. All the data shown is for the 30% glycerol system at T = 310 K. Colour is consistent throughout the figure.

As well as calculating the location of glycerol within the DPPC bilayers and monolayers, we can also calculate the regions of the DPPC molecules with which glycerol will form interactions within the solvent phase of the simulation box. Overall, in all situations, glycerol interactions are predominately observed to occur from the solvent phase with the choline headgroup of the lipid, which is to be expected as it is the closest region to the solvent (figure 6B – D). Fewer interactions are noted for the ester region (analysed for the double bonded oxygen atom region) than that of the phosphate group (phosphate oxygen atoms), which is also to be expected as that region is further away from the solvent and thus the glycerol molecules.

Effect of Glycerol on the Structure of DPPC Monolayers & Bilayers

As the percentage of glycerol was increased within the water phase of the simulation box for both monolayer and bilayer systems, the calculated area per lipid of DPPC increased (from ~53 to 59 $Å^2$ for the bilayer, and 57 to 59 $Å^2$ for the monolayer, figure 7A). The initial difference in area is due to the compression of the simulation box as the bilayer simulation is pressure coupled within the x and y dimensions independently of the z (semi-isotropically to 1 bar). This does not occur within the monolayer simulations due to an NVT ensemble being utilised, thus a different box size and area per lipid is present at the start. These increases are in agreement with the experimentally calculated area per lipids (from area expansion) from surface pressure area isotherms presented

earlier (figure 2), indicating that as the amount of glycerol within the solvent phase increases, the "larger" the lipid becomes.

Also calculated from simulation is the thickness of DPPC in both bilayer (phosphate to phosphate distance) and monolayer systems (from the phosphate headgroup to the terminal carbon within the lipid tails). Within figure 7B, the "length" of the DPPC lipid does decrease with the addition of glycerol. This trend of lipid thinning is in agreement with the SANS calculations reported in Table 3 and supporting the hypothesis that the more glycerol there is present in the solvent phase, the thinner the DPPC lipid becomes. The mechanism by which this thinning occurs shall be discussed later (in regards to simulations), however these results suggest that the hypothesis that intercalation of lipid tails is the cause of the thinning of the membranes is not observed or proved in these simulations.

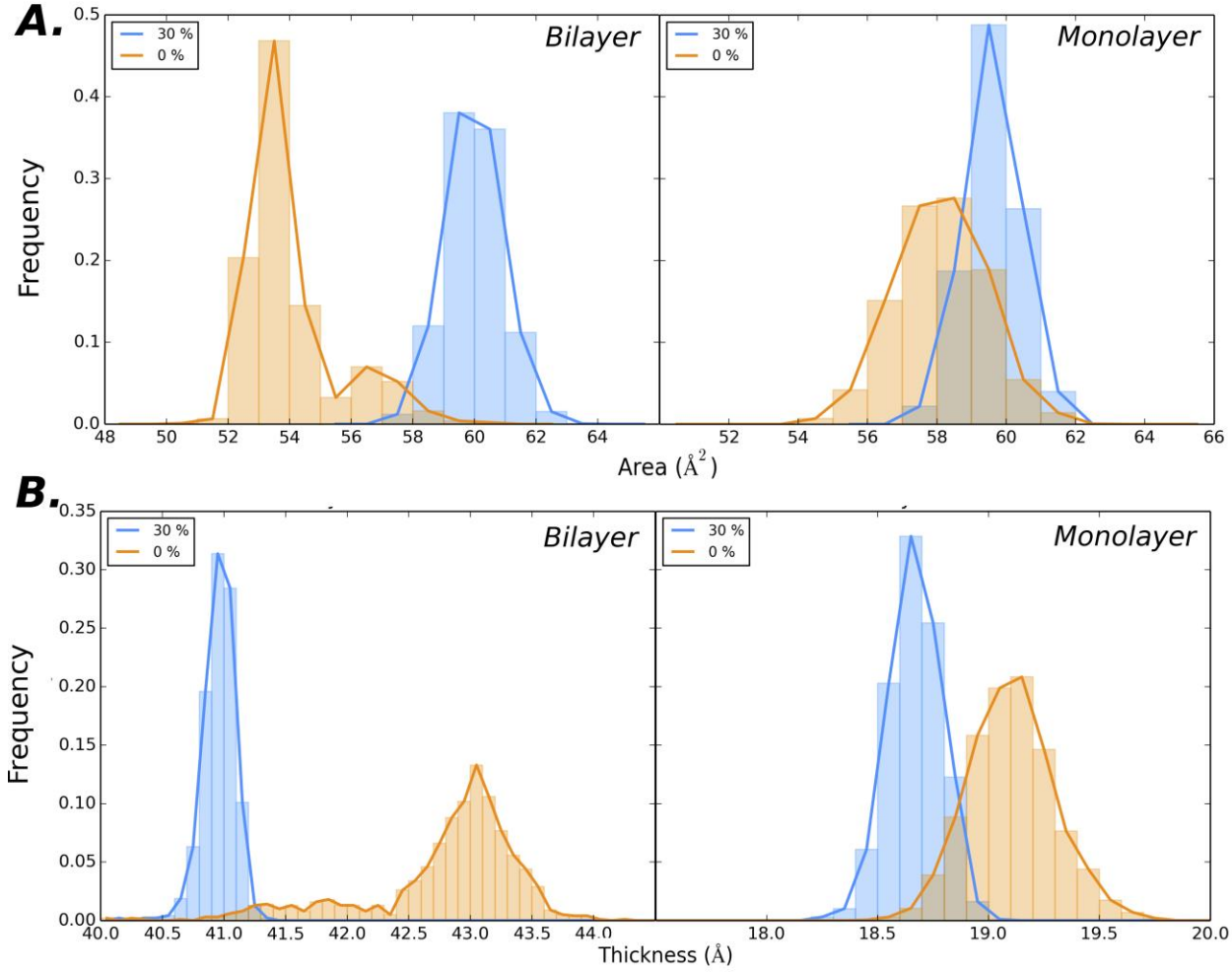

Figure 7. (A) Distribution of the area per lipid for the bilayer (left) and monolayer systems (right) at 0% w/w glycerol (orange) and 30% w/w glycerol (blue). Initial areas differ due to box set up (discussed in main text). **(B)** Distribution of the thickness of the bilayer (left) and monolayer (right) at 0% w/w glycerol (orange) and 30% w/w glycerol (blue).

The calculation of the headgroup angle suggests that the bilayer/monolayer thinning observed with the addition of glycerol experimentally and in simulation is due to the change in the headgroup angle of the lipid. As the percentage of glycerol in solution increases, the lipid headgroup becomes more parallel to the membrane surface therefore presenting a smaller (in regards to height), DPPC lipid. This can be supported from the MD data (figure 8) which shows that at both the gel and

liquid crystalline temperatures of DPPC, the distribution of lipid angles decreases as the glycerol percentage increases which could be accountable for the small change in thickness noted earlier.

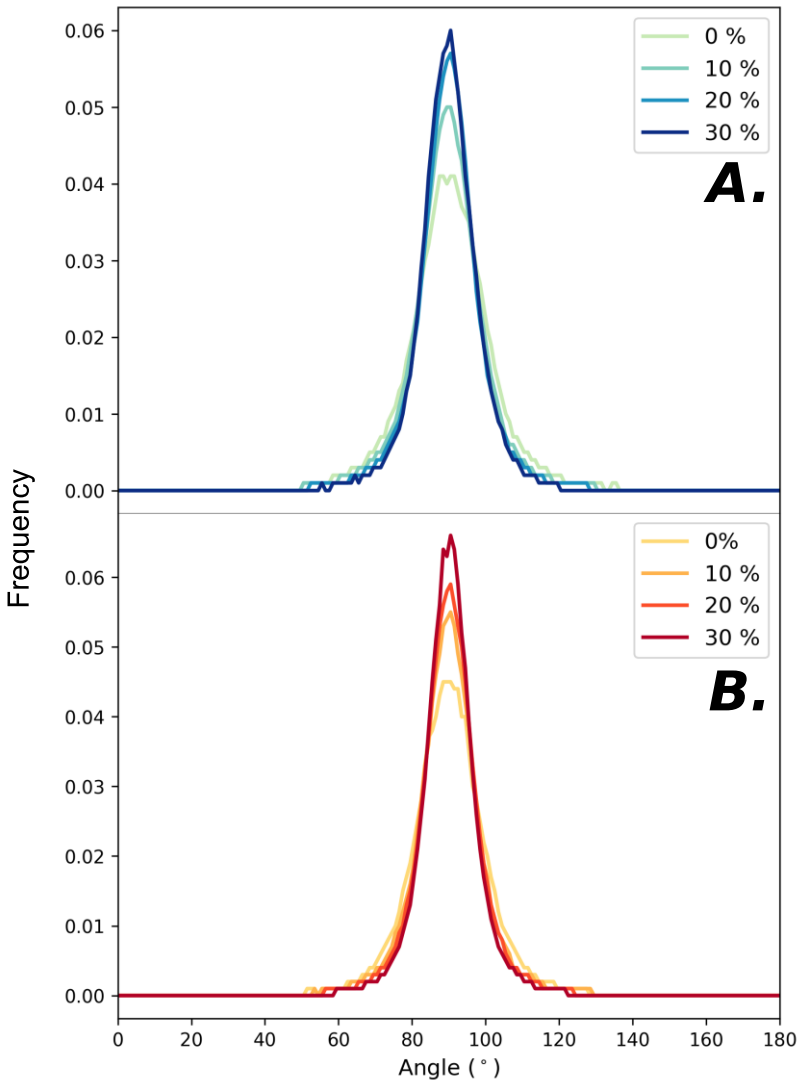

Figure 8. Distrubution of the headgroup angle of DPPC lipids (phosphate to choline group angle, with 0 degrees indicating the lipid is parallel to the z plane and 90 the lipid is pararell to the monolayer) for a monolayer simulation at 310 K **(A)** and 323 K **(B)** with varying glycerol percentages (indicated in figure).

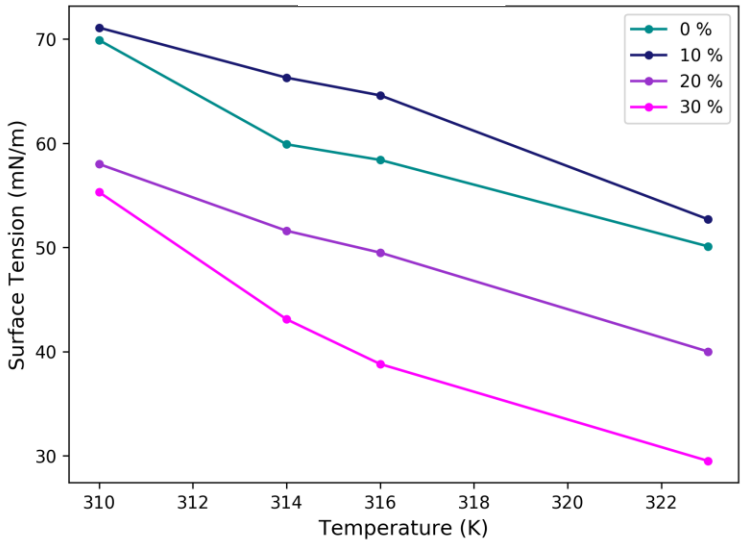

Figure 9. Surface tension as a function of temperature and glycerol concentration. The data is from the DPPC monolayer simulations.

Finally, from the MD simulations, the surface tension of the lipid monolayer can also be calculated. This has been shown previously to decrease with the addition of alcohols to the water phase[55] and here a similar effect is being noted with glycerol addition. When glycerol is present in the monolayer systems, the surface tension measured in our simulations is observed to decrease as the concentration of glycerol increases at each temperature that has been studied (figure 9). This modification of the surface tension as a result of the membranes interaction with glycerol could have an interesting effect *in vivo* within the lung lining and the transport of drugs through the pulmonary surfactant.

DISCUSSION

The putative stiffening effects of glycerol on gel phase lipid-based models of pulmonary interfaces have been attributed to preferential glycerol localisation at the interfacial region, observed using both X-ray and neutron reflectivity techniques[15]. An increased concentration of

headgroup-associated glycerol might be expected to lead to an increase in glycerol-mediated hydrogen bonding in the interfacial region, effectively making lipid bilayers more viscous and thus mechanically stiffer. This theoretical construct appears to be at odds with the evidence from studies which demonstrate that association of glycerol with DPPC increases the size of the lipid headgroup and causes expansion of lipid lamellae due to an increase in steric repulsion[21], which suggests a disordering effect on lipid chain packing. We sought to resolve this apparent contradiction by a detailed examination of the molecular interactions between DPPC and glycerol, through a combination of physicochemical measurements on gel phase lipids and *in silico* simulations which additionally examined the effects of increased temperature and the presence of salts.

The molecular interactions between glycerol and DPPC were elucidated by comparing the FTIR results with data obtained using MD simulations. Investigations were focussed on four FTIR spectral regions which represent both the hydrophilic and hydrophobic parts of the phospholipid molecules. With respect to the DPPC headgroup, the carbonyl, phosphate, and choline moieties were investigated for alteration in hydration. The carbonyl stretching band between 1800 and 1600 cm^{-1} represents the ester carbonyl groups present at the interfacial region. In fully hydrated bilayers, generally, this band can be divided into two ranges; a high wavenumber (~1742 cm^{-1}) and a low wavenumber (~1728 cm^{-1}) corresponding to the non-hydrogen bonded and hydrogen bonded C=O groups, respectively[45]. In the presence of glycerol, the relative intensity of the non-hydrogen bonded C=O band increased from 1732.7 to 1738.9 cm^{-1} compared to that of the DPPC liposomes in ultrapure water, indicating that dehydration at the interfacial region was enhanced by glycerol, thus the presence of glycerol reduced hydrogen bond formation between solvent and the carbonyl oxygen of DPPC. This effective dehydration of the interfacial carbonyl groups was also observed in the MD simulations for DPPC monolayers and bilayers. The simulations also

suggested that the vast majority of the glycerol in the system is associated with the lipid headgroup, with little located in the lipid acyl chain region.

Although the formation of hydrogen bonds with the phosphate group was detected by FTIR in the presence of glycerol, the spectra remained similar to those obtained from glycerol-free DPPC dispersions. Therefore, it was not possible to differentiate water from glycerol hydrogen bonding with the phosphate of DPPC. With respect to solvent interactions with the headgroup phosphate, the data from the MD simulations was more enlightening, suggesting that water molecules preferentially locate in the region of the headgroup. This may explain why, even at high glycerol concentrations, some water remains detectably associated with the DPPC headgroup[15]. Overall, the simulations showed that glycerol interacts primarily with the choline moiety of the DPPC headgroup, and that glycerol molecules are able to form associations between neighbouring choline groups, thus effectively cross-linking the lipid headgroups. This preferential localisation of glycerol around the quaternary ammonium was also evident from the FTIR data which shows that the $N(CH_3)_3^+$ asymmetric stretching shifts towards higher wavenumbers than ~970 cm^{-1} in the hydrogen bonded region[46] and indicated a bending of the choline moiety towards the plane of the membrane surface[47], the significance of which is discussed below.

Aside from the hydrophilic regions of the DPPC molecule, FTIR was also used to examine the vibrational frequencies of the methylene and the terminal methyl stretching bands, parameters which are commonly used to detect the conformational changes in and mobility of the hydrocarbon chain[22,45]. Although there was no difference in the methylene stretching region when glycerol was present in the liposomal system, the observed shift in the wavenumber of terminal methyl stretching mode indicated a restriction of the terminal methyl movement. It can therefore be implied that glycerol did not penetrate into the hydrophobic core of the DPPC bilayers, but the

influence that it has on the polar region may affect the ordering of the hydrophobic chains. The strong hydrophilicity of glycerol and its consequent tendency to remain associated with the DPPC headgroup may explain why it does not have a disordering effect on the lipid, unlike molecules such as propylene glycol which can readily penetrate into hydrophobic core of PC bilayers and cause destabilisation at concentrations as low as 10% v/v in aqueous solution[56].

The ways in which the various interactions between glycerol and the DPPC headgroup affect the physical properties of the lipid lamellae in both monolayers and bilayers, were also investigated using experimental and *in silico* simulation methods. The preferential association of glycerol with different PC headgroup moieties increased the volume of the solvation shell and led to the increase in DPPC monolayer area per molecule observed in previous studies[57–59] and in our Langmuir isotherm data and simulations. In DPPC bilayers, this increase in area per molecule can lead to a lateral expansion of the lipid lamellae which is compensated for by the formation of an interdigitated phase, previously reported for DPPC bilayers formed in perdeuterated glycerol[60]. However, neither the DPPC vesicle SANS data, nor the bilayer simulations carried out for this study showed any evidence of this occurring in 30% glycerol solutions. What was observed in both SANS fitting and MD simulations was a small but significant ~3 Å decrease in bilayer thickness in 30% glycerol compared to pure water. The most likely explanation for this membrane thinning, is that the presence of glycerol causes the choline headgroup to orientate parallel to the plane of the bilayer, whereas in the gel phase it would adopt a more perpendicular orientation[21]. Evidence for this comes from the FTIR measurements which show an increase in the intensity of the choline band, implying that glycerol induced hydrogen bonding bends this group from perpendicular to a parallel arrangement with respect to the membrane plane. Additionally, as glycerol was introduced into our simulation systems, the headgroups of the lipids assumed an

orientation which was more parallel to membrane surface. This may mean that some areas of LE phase exist in the gel phase bilayers[21], which would explain why a glycerol concentration dependent decrease in the surface compressional modulus of DPPC monolayers was observed at 30 mN/m.

Alterations in lipid bilayer packing, such as those caused by the glycerol-induced headgroup alterations observed for DPPC, can affect the thermotropic phase behaviour of the phospholipids, which we investigated using fluorimetry. In this study, the changes in Laurdan GP[26], over the temperature range of 35°C to 45°C, provided evidence for a glycerol-induced modification of membrane phase behaviour, indicating a modest but significant increase in the DPPC MLV T_m from ~41.2°C in water, to 42.8°C in 30.0% w/w glycerol. Although it has previously been demonstrated that preferential solvation of DPPC by sugars causes headgroup dehydration and a subsequent increase in T_m [61], similar to that we have observed, the glycerol-induced increase in T_m has not previously been found to be significant[60]. Nevertheless, it remains intriguing that the observed monolayer expansion caused by headgroup solvation by glycerol did not result in significant disordering of the lipid bilayers and thus a reduction in T_m. As the SANS results suggest, the headgroup expansion does not lead to a compensation in chain packing such as interdigitation, and therefore to extend this study, some higher resolution techniques such as X-ray or neutron reflectometry and IRRAS on planar models, could provide useful complementary data on the effects of headgroup/glycerol interaction on chain packing as the lipids undergo their melting transition.

The impact of these glycerol induced bilayer changes on solute permeability can be expected to depend on epithelial transport mechanism which is determined by the molecular properties of an inhaled drug. The hypothesis that membrane stiffening demonstrated herein contributes to the

reduced transport of beclomethasone dipropionate delivered to lung epithelial cells in glycerol-containing particles in previous studies[5–7] provides a starting point for further investigation.

CONCLUSION

Collectively, our data shows that glycerol localises preferentially around the carbonyls and quaternary ammonium of the DPPC headgroup and has the potential to form cross-links between headgroups. The subsequent expansion of the lipid molecular area and changing the orientation of choline in the gel phase cause an alteration in bilayer structure. These changes constrain the acyl chains and alter lipid order (but do not greatly affect T_m), which may in turn result in the stiffening of the membrane[15]. The combination of the localised glycerol adlayer and consequent bilayer packing alteration has the potential to affect the partitioning and uptake kinetics of steroidal drugs such as BDP. The experimental and simulated monolayer and bilayer model systems we have characterised will provide a useful platform for examining the effect of glycerol-induced membrane structure alterations on inhaled drug permeability.

ASSOCIATED CONTENT

Supporting Information Available: Figure S1, Temperature dependence of the effect of glycerol 0 – 30% w/w on the Laurdan GP in DPPC MLVs. Figure S2, SANS scattering vector versus intensity curves (unfilled symbols) and their associated paracrystalline lamellar stack model fits (solid lines) for d_{62}DPPC vesicles dispersed in H_2O and 30% w/w glycerol solution, at 25°C. This material is available free of charge via the Internet at http://pubs.acs.org.

AUTHOR INFORMATION

Corresponding Author

*Tel.: +44 (0)207 848 4823. E-mail address: ben.forbes@kcl.ac.uk (Ben Forbes).

Present Addresses

[1] School of Cancer and Pharmaceutical Sciences, King's College London, London, SE1 9NH, UK

[2] Department of Physics, King's College London, London, WC2R 2LS, UK.

[3] Rutherford Appleton Laboratory, ISIS Facility, Chilton, Oxfordshire, OX11 0QX, UK.

[4] Institute of Pharmacy, Martin-Luther-University Halle-Wittenberg, Halle (Saale), 06099, Germany.

Author Contributions

The manuscript was written through contributions of all authors: Wachirun Terakosolphan. Author-One, Dr Jemma L. Trick. Author-Two, Dr Paul G. Royall. Author-Three, Dr Sarah E. Rogers. Author-Four, Olimpia Lamberti. Author-Five, Dr Christian D. Lorenz. Author-Six, Prof Ben Forbes. Author-Seven (Corresponding Author*), and Dr Richard D. Harvey. Author-Eight. All authors have given approval to the final version of the manuscript. These authors contributed equally.

Funding Sources

- Government Pharmaceutical Organization of Thailand (W. Terakosolphan)

Notes

The authors declare no competing financial interest.

ACKNOWLEDGMENT

The authors are sincerely grateful to all kind help from School of Cancer and Pharmaceutical Sciences, King's College London, for the specific experiments we used in this study; Dr Andrew Chan and Mr Abdulrahman Aloumi for FTIR, and Ms Kalliopi-Kelli Vandera for Langmuir isotherms. Through Chris Lorenz's membership within the UK HPC Materials Chemistry Consortium, which is funded by the Office of Science and Technology through the EPSRC High End Computing Programme (Grant No. EP/L000202), we were able to use the facilities of ARCHER, the UK National Supercomputing Service (http://www.archer.ac.uk), to carry out aspects of this work. Also, some of the simulations were conducted using computational time on the MareNostrum supercomputer, which was generously provided by the Barcelona Supercomputing Center through a grant from Red Española de Supercomputación. Lastly, Mr Wachirun Terakosolphan has been supported by a PhD scholarship from the Government Pharmaceutical Organization of Thailand.

ABBREVIATIONS

BDP, beclomethasone dipropionate; DPPC, dipalmitoylphosphatidylcholine; FTIR, fourier transform infrared spectroscopy; SANS, small angle neutron scattering; MD, molecular dynamics simulation; T_m, gel to fluid phase transition temperature; APM, area per molecule; K^s, surface compressional modulus; GP, generalised polarisation.

REFERENCES

(1) Karbowiak, T.; Hervet, H.; Léger, L.; Champion, D.; Debeaufort, F.; Voilley, A. Effect of Plasticizers (Water and Glycerol) on the Diffusion of a Small Molecule in Iota-Carrageenan Biopolymer Films for Edible Coating Application. *Biomacromolecules* **2006**, *7* (6), 2011–

2019.

(2) Suchomel, M.; Weinlich, M.; Kundi, M. Influence of Glycerol and an Alternative Humectant on the Immediate and 3-Hours Bactericidal Efficacies of Two Isopropanol-Based Antiseptics in Laboratory Experiments in Vivo according to EN 12791. *Antimicrob. Resist. Infect. Control* **2017**, *6* (1), 4–8.

(3) Koseki, T.; Koganezawa, M.; Furuyama, A.; Isono, K.; Shimada, I. A Specific Receptor Site for Glycerol, a New Sweet Tastant for Drosophila: Structure-Taste Relationship of Glycerol in the Labellar Sugar Receptor Cell. *Chem. Senses* **2004**, *29* (8), 703–711.

(4) Brambilla, G.; Ganderton, D.; Garzia, R.; Lewis, D.; Meakin, B.; Ventura, P. Modulation of Aerosol Clouds Produced by Pressurised Inhalation Aerosols. *Int. J. Pharm.* **1999**, *186* (1), 53–61.

(5) Grainger, C. I.; Saunders, M.; Buttini, F.; Telford, R.; Merolla, L. L.; Martin, G. P.; Jones, S. A.; Forbes, B. Critical Characteristics for Corticosteroid Solution Metered Dose Inhaler Bioequivalence. *Mol. Pharm.* **2012**, *9* (3), 563–569.

(6) Lewis, D. A.; Young, P. M.; Buttini, F.; Church, T.; Colombo, P.; Forbes, B.; Haghi, M.; Johnson, R.; O'Shea, H.; Salama, R.; et al. Towards the Bioequivalence of Pressurised Metered Dose Inhalers 1: Design and Characterisation of Aerodynamically Equivalent Beclomethasone Dipropionate Inhalers with and without Glycerol as a Non-Volatile Excipient. *Eur. J. Pharm. Biopharm.* **2014**, *86* (1), 31–37.

(7) Haghi, M.; Bebawy, M.; Colombo, P.; Forbes, B.; Lewis, D. A.; Salama, R.; Traini, D.; Young, P. M. Towards the Bioequivalence of Pressurised Metered Dose Inhalers 2 .

Aerodynamically Equivalent Particles (with and without Glycerol) Exhibit Different Biopharmaceutical Profiles in Vitro. *Eur. J. Pharm. Biopharm.* **2014**, *86*, 38–45.

(8) Hastedt, J. E.; Bäckman, P.; Clark, A. R.; Doub, W.; Hickey, A.; Hochhaus, G.; Kuehl, P. J.; Lehr, C.-M.; Mauser, P.; McConville, J.; et al. Scope and Relevance of a Pulmonary Biopharmaceutical Classification System AAPS/FDA/USP Workshop March 16-17th, 2015 in Baltimore, MD. *AAPS Open* **2016**, *2* (1), 1–20.

(9) Derendorf, H.; Hochhaus, G.; Meibohm, B.; Möllmann, H.; Barth, J. Pharmacokinetics and Pharmacodynamics of Inhaled Corticosteroids. *J. Allergy Clin. Immunol.* **1998**, *101*, S440–S446.

(10) Olsson, B.; Bondesson, E.; Borgström, L.; Edsbäcker, S.; Ekelund, K.; Gustavsson, L.; Hegelund-myrbäck, T. Pulmonary Drug Metbolism, Clearance, and Absorption. In *Controlled Pulmonary Drug Delivery*; Smyth, H. D. C., Hickey, A. J., Eds.; Springer: New York, 2011; pp 21–50.

(11) Martinelli, F.; Balducci, A. G.; Kumar, A.; Sonvico, F.; Forbes, B.; Bettini, R.; Buttini, F. Engineered Sodium Hyaluronate Respirable Dry Powders for Pulmonary Drug Delivery. *Int. J. Pharm.* **2017**, *517* (1–2), 286–295.

(12) Ashiru-Oredope, D. A. I.; Patel, N.; Forbes, B.; Patel, R.; Basit, A. W. The Effect of Polyoxyethylene Polymers on the Transport of Ranitidine in Caco-2 Cell Monolayers. *Int. J. Pharm.* **2011**, *409* (1–2), 164–168.

(13) Parr, A.; Hidalgo, I. J.; Bode, C.; Brown, W.; Yazdanian, M.; Gonzalez, M. A.; Sagawa, K.; Miller, K.; Jiang, W.; Stippler, E. S. The Effect of Excipients on the Permeability of BCS

Class III Compounds and Implications for Biowaivers. *Pharm. Res.* **2016**, *33* (1), 167–176.

(14) Vasconcelos, T.; Marques, S.; Sarmento, B. The Biopharmaceutical Classification System of Excipients. *Ther. Deliv* **2017**, *8* (2), 65–78.

(15) Pocivavsek, L.; Gavrilov, K.; Cao, K. D.; Chi, E. Y.; Li, D.; Lin, B.; Meron, M.; Majewski, J.; Lee, K. Y. C. Glycerol-Induced Membrane Stiffening: The Role of Viscous Fluid Adlayers. *Biophys. J.* **2011**, *101* (1), 118–127.

(16) Bhatia, S. K. *Biomaterials for Clinical Applications*; Springer: New York, 2010.

(17) Goerke, J. Pulmonary Surfactant : Functions and Molecular Composition. *Biochim. Biophys. Acta* **1998**, *1408*, 79–89.

(18) Matyszewska, D.; Bilewicz, R. DPPC Monolayers as Simple Models of Biological Membranes for Studies of Interactions with Perfluorinated Compounds. *Ann. Univ. Mariae Curie, Chem.* **2008**, *63* (16), 201–210.

(19) Wójtowicz, K. Effect of Some Pharmaceuticals on DPPC Membranes Phase Transition — Ultrasound Absorption Study. *Instrum. Sci. Technol.* **1999**, *24* (4), 287–293.

(20) Pocivavsek, L.; Frey, S. L.; Majewski, J.; Kjaer, K.; Lee, K. Y. C. Effect of Aqueous Glycerol Subphases on DPPC : POPG 7 : 3 Packing. **2006**, 1123–1124.

(21) Brumm, T.; Naumann, C.; Sackmann, E.; Bayed, T. M. Conformational Changes of the Lecithin Headgroup in Monolayers at the Air/water Interface. *Eur. Biophys. J.* **1994**, *23*, 289–295.

(22) Toyran, N.; Severcan, F. Infrared Spectroscopic Studies on the Dipalmitoyl

Phosphatidylcholine Bilayer Interactions with Calcium Phosphate: Effect of Vitamin D2. *Spectroscopy* **2002**, *16*, 399–408.

(23) Umemura, J.; Cameron, D. G.; Mantsch, H. H. A Fourier Transform Infrared Spectroscopic Study of The Molecular Interaction of Cholesterol with 1,2-Dipalmitoyl-Sn-Glycero-3-Phosphocholine. *Biochim. Biophys. Acta* **1980**, *602*, 32–44.

(24) Hohlfeld, J. M. The Role of Surfactant in Asthma. *Respir. Res.* **2002**, *3*, 4.

(25) Dynarowicz-Łatka, P.; Hac-Wydro, K. Interactions between Phosphatidylcholines and Cholesterol in Monolayers at the Air/water Interface. *Colloids Surfaces B Biointerfaces* **2004**, *37* (1–2), 21–25.

(26) Harris, F. M.; Best, K. B.; Bell, J. D. Use of Laurdan Fluorescence Intensity and Polarization to Distinguish between Changes in Membrane Fluidity and Phospholipid Order. *Biochim. Biophys. Acta* **2002**, *1565*, 123–128.

(27) Parasassi, T.; Stasio, G. De; D'Ubaldo, A.; Gratton, E. Phase Fluctuation in Phospholipid Membranes Revealed by Laurdan Fluorescence. *Biophys. J.* **1990**, *57* (6), 1179–1186.

(28) Parasassi, T.; Stasio, G. De; Ravagnan, G.; Rusch, R. M.; Gratton, E. Quantitation of Lipid Phases in Phospholipid Vesicles by the Generalized Polarization of Laurdan Fluorescence. *Biophys. J.* **1991**, *60*, 179–189.

(29) Rodríguez, G.; Cócera, M.; Rubio, L.; Alonso, C.; Pons, R.; Sandt, C.; Dumas, P.; López-Iglesias, C.; de la Maza, A.; López, O. Bicellar Systems to Modify the Phase Behaviour of Skin Stratum Corneum Lipids. *Phys. Chem. Chem. Phys.* **2012**, *14* (42), 14523.

(30) Science and Technology Facilities Council. ISIS Neutron and Muon Source https://www.isis.stfc.ac.uk/Pages/home.aspx.

(31) Heenan, R. K.; Penfold, J.; King, S. M. SANS at Pulsed Neutron Sources: Present and Future Prospects. *J. Appl. Crystallogr.* **1997**, *30*, 1140–1147.

(32) Mantid. Manipulation and Analysis Toolkit for Instrument Data. http://dx.doi.org/10.5286/SOFTWARE/MANTID.

(33) Wignall, G. D.; Bates, F. S. Absolute Calibration of Small-Angle Neutron Scattering Data. *J. Appl. Crystallogr.* **1987**, *20*, 28–40.

(34) Bergström, M.; Pedersen, J. S.; Schurtenberger, P.; Egelhaaf, S. Small-Angle Neutron Scattering (SANS) Study of Vesicles and Lamellar Sheets Formed from Mixtures of an Anionic and a Cationic Surfactant. *J. Phys. Chem. B* **1999**, *103* (45), 9888–9897.

(35) Butler, P.; Alina, G.; Hernandez, R. C.; Doucet, M.; Jackson, A.; Kienzle, P.; Kline, S.; Zhou, J. SASView for Small Angle Scattering Analysis. http://www.sasview.org/.

(36) Wu, E. L.; Cheng, X.; Jo, S.; Rui, H.; Song, K. C.; Dávila-Contreras, E. M.; Qi, Y.; Lee, J.; Monje-Galvan, V.; Venable, R. M.; et al. CHARMM-GUI Membrane Builder toward Realistic Biological Membrane Simulations. *J. Comput. Chem.* **2014**, *35* (27), 1997–2004.

(37) Abraham, M. J.; Murtola, T.; Schulz, R.; Páall, S.; Smith, J. C.; Hess, B.; Lindah, E. Gromacs: High Performance Molecular Simulations through Multi-Level Parallelism from Laptops to Supercomputers. *SoftwareX* **2015**, *1–2*, 19–25.

(38) Klauda, J. B.; Venable, R. M.; Freites, J. A.; O'Connor, J. W.; Tobias, D. J.; Mondragon-

Ramirez, C.; Vorobyov, I.; MacKerell, A. D.; Pastor, R. W. Update of the CHARMM All-Atom Additive Force Field for Lipids: Validation on Six Lipid Types. *J. Phys. Chem. B* **2010**, *114* (23), 7830–7843.

(39) Nosé, S. A Unified Formulation of the Constant Temperature Molecular Dynamics Methods. *J. Chem. Phys.* **1984**, *81* (1), 511.

(40) Parrinello, M.; Rahman, a. Polymorphic Transitions in Single Crystals: A New Molecular Dynamics Method. *J. Appl. Phys.* **1981**, *52* (12), 7182–7190.

(41) Darden, T.; York, D.; Pedersen, L. Particle Mesh Ewald: An Nlog(N) Method for Ewald Sums in Large Systems. *J. Chem. Phys.* **1993**, *98* (12), 10089–10091.

(42) Michaud-Agrawal, N.; Denning, E. J.; Woolf, T. B.; Beckstein, O. MDAnalysis: A Toolkit for the Analysis of Molecular Dynamics Simulations. *J. Comput. Chem.* **2011**, *32* (10), 2319–2327.

(43) Lewis, R. N.; Mannock, D. A.; McElhaney, R. N.; Wong, P. T.; Mantsch, H. H. Physical Properties of Glycosyldiacylglycerols: An Infrared Spectroscopic Study of the Gel-Phase Polymorphism of 1,2-Di-O-Acyl-3-O-(Beta-D-Glucopyranosyl)-Sn-Glycerols. *Biochemistry* **1990**, *29* (38), 8933–8943.

(44) López-García, F.; Micol, V.; Villalaín, J.; Gómez-Fernández, J. C. Infrared Spectroscopic Study of the Interaction of Diacylglycerol with Phosphatidylserine in the Presence of Calcium. *Biochim. Biophys. Acta (BBA)/Lipids Lipid Metab.* **1993**, *1169* (3), 264–272.

(45) Berényi, S.; Mihály, J.; Kristyán, S.; Naszályi Nagy, L.; Telegdi, J.; Bóta, A. Thermotropic

and Structural Effects of Poly(malic Acid) on Fully Hydrated Multilamellar DPPC-Water Systems. *Biochim. Biophys. Acta - Biomembr.* **2013**, *1828* (2), 661–669.

(46) Popova, A. V; Hincha, D. K. Intermolecular Interactions in Dry and Rehydrated Pure and Mixed Bilayers of Phosphatidylcholine and Digalactosyldiacylglycerol: A Fourier Transform Infrared Spectroscopy Study. *Biophys. J.* **2003**, *85* (3), 1682–1690.

(47) Le Saux, A.; Ruysschaert, J.-M.; Goormaghtigh, E. Membrane Molecule Reorientation in an Electric Field Recorded by Attenuated Total Reflection Fourier-Transform Infrared Spectroscopy. *Biophys. J.* **2001**, *80* (1), 324–330.

(48) Romero, C. M.; Paéz, M. S. Surface Tension of Aqueous Solutions of Alcohol and Polyols at 298.15 K. *Phys. Chem. Liq.* **2006**, *44* (1), 61–65.

(49) Åkesson, A.; Lind, T.; Ehrlich, N.; Stamou, D.; Wacklin, H.; Cárdenas, M. Composition and Structure of Mixed Phospholipid Supported Bilayers Formed by POPC and DPPC. *Soft Matter* **2012**, *8*, 5658.

(50) Immirzi, A.; Perini, B. Prediction of Density in Organic Crystals. *Acta Crystallogr. Sect. A* **1977**, *33* (1), 216–218.

(51) Harvey, R. D.; Heenan, R. K.; Barlow, D. J.; Lawrence, M. J. The Effect of Electrolyte on the Morphology of Vesicles Composed of the Dialkyl Polyoxyethylene Ether Surfactant 2C 18E 12. *Chem. Phys. Lipids* **2005**, *133* (1), 27–36.

(52) Nagle, J. F.; Tristram-Nagle, S. Structure of Lipid Bilayers. *Biochim. Biophys. Acta - Rev. Biomembr.* **2000**, *1469* (3), 159–195.

(53) Ipsen, J. H.; Mouritsen, O. G.; Bloom, M. Relationships between Lipid-Membrane Area, Hydrophobic Thickness, and Acyl-Chain Orientational Order -- The Effects of Cholesterol. *Biophys. J.* **1990**, *57* (3), 405–412.

(54) Allen, D. T.; Saaka, Y.; Pardo, L. C.; Lawrence, M. J.; Lorenz, C. D.; Paria, S.; Khilar, K. C.; Lawrence, M. J.; Rees, G. D.; Rabinow, B. E.; et al. Specific Effects of Monovalent Counterions on the Structural and Interfacial Properties of Dodecyl Sulfate Monolayers. *Phys. Chem. Chem. Phys.* **2016**, *18* (44), 30394–30406.

(55) Vazquez, G.; Alvarez, E.; Navaza, J. M. Surface Tension of Alcohol + Water from 20 to 50 °C. *J. Chem. Eng. Data* **1995**, *40* (3), 611–614.

(56) Harvey, R. D.; Ara, N.; Heenan, R. K.; Barlow, D. J.; Quinn, P. J.; Lawrence, M. J. Stabilization of Distearoylphosphatidylcholine Lamellar Phases in Propylene Glycol Using Cholesterol. *Mol. Pharm.* **2013**, *10* (12), 4408–4417.

(57) Maggio, B. B.; Ahkong, Q. F. A. H.; Lucy, J. A. Poly(Ethylene Glycol), Surface Potential and Cell Fusion. *Biochem. J.* **1976**, *158* (3), 647–650.

(58) Crowe, J. H.; Whittam, M. A.; Chapman, D.; Crowe, L. M. Interactions of Phospholipid Monolayers with Carbohydrates. *Biochim. Biophys. Acta* **1984**, *769*, 151–159.

(59) Clark, G. A.; Henderson, J. M.; Heffern, C.; Akgün, B.; Majewski, J.; Lee, K. Y. C. Synergistic Interactions of Sugars/Polyols and Monovalent Salts with Phospholipids Depend upon Sugar/Polyol Complexity and Anion Identity. *Langmuir* **2015**, *31* (46), 12688–12698.

(60) O'Leary, T. J.; Levin, I. W. Raman Spectroscopic Study of an Interdigitated Lipid Bilayer. Dipalmitoylphosphatidylcholine Dispersed in Glycerol. *BBA - Biomembr.* **1984**, *776* (2), 185–189.

(61) Crowe, L. M.; Crowe, J. H. Solution Effects on the Thermotropic Phase Transition of Unilamellar Liposomes. *BBA - Biomembr.* **1991**, *1064* (2), 267–274.

Abstract Graphic